



Crystallization behavior of poly(L-lactic acid) affected by the addition of a small amount of poly(3-hydroxybutyrate)

Yun Hu^a, Harumi Sato^a, Jianming Zhang^{a,b}, Isao Noda^c, Yukihiro Ozaki^{a,*}

^aDepartment of Chemistry, School of Science and Technology, and Research Center for Environment Friendly Polymers, Kwansei-Gakuin University, Gakuen, Sanda 669-1337, Japan

^bKey Laboratory of Rubber-plastics, Ministry of Education, Department of Polymer Science and Engineering, Qingdao University of Science and Technology, Qingdao City 266042, People's Republic of China

^cThe Procter & Gamble Company, 8611 Beckett Road, West Chester, OH 45069, USA

ARTICLE INFO

Article history:

Received 20 January 2008

Received in revised form 3 July 2008

Accepted 19 July 2008

Available online 25 July 2008

Keywords:

Poly(3-hydroxybutyrate)/poly(L-lactic acid) blends

Crystallization

Infrared spectroscopy

ABSTRACT

The miscibility, crystallization and subsequent melting behavior in binary biodegradable polymer blends of poly(L-lactic acid) (PLLA) and low molecular weight poly(3-hydroxybutyrate) (PHB) have been investigated by differential scanning calorimetry (DSC), Fourier-transform infrared (FTIR) spectroscopy, and wide-angle X-ray diffraction (WAXD). DSC analysis results indicated that PLLA showed no miscibility with high molecular weight PHB ($M_w = 650,000 \text{ g mol}^{-1}$) in the 80/20, 60/40, 40/60, 20/80 composition range of the PHB/PLLA blends. On the other hand, it showed some limited miscibility with low molecular weight PHB ($M_w = 5000 \text{ g mol}^{-1}$) when the PHB content was below 25%, as evidenced by small changes in the glass transition temperature of PLLA. The partial miscibility was further supported by changes of cold-crystallization behavior of PLLA in the blends. During the nonisothermal crystallization, it was found that the addition of a small amount of PHB up to 30% made the cold-crystallization of PLLA occur in the lower temperature. Meanwhile, the crystallization of PHB and PLLA was observed in the heating process by monitoring characteristic IR bands of each component for the low molecular weight PHB/PLLA 20/80 and 30/70 blends. The temperature-dependent IR and WAXD results also revealed that for PLLA component crystallization, the disorder (α') phase of PLLA was produced, and that the α' phase changed to the order (α) phase just prior to the melting point.

© 2008 Elsevier Ltd. All rights reserved.

1. Introduction

In the last decade, considerable attention has been paid to the biodegradable and biocompatible polymers, because they are produced from renewable resources and biodegraded back to water and carbon dioxide after use [1–6]. Poly(3-hydroxybutyrate) (PHB) is one of the most well-known biosynthesized and biodegradable aliphatic polyesters and has been extensively studied by many research groups. However, PHB has some shortcomings, for example, high crystallinity, brittleness and narrow processing window, which have prevented its potential applications. To reduce its excess crystallinity and improve the mechanical properties of PHB, blending with other polymers is considered to be an easy and cost-effective way [6–21].

PHB blended with poly(L-lactic acid) (PLLA) has been attracting significant interests, because both of them are biodegradable. Therefore, a considerable number of research works have been focused on the investigations of the miscibility, crystallization,

melting behavior, and solid-state structures of PHB/PLLA blends, with the aim of improving their mechanical properties and the utility in practical applications [12–21]. Previous studies on PHB/PLLA blends showed that the miscibility between these two polymers is dependent on the molecular weight of the second component [12–16]. PHB is miscible with low molecular weight PLLA ($M_w < 18,000$) in the melt over the whole composition range, whereas the PHB blends with high molecular weight PLLA ($M_w > 18,000$) show biphasic separation [12–14]. Similarly, the PLLA component is miscible with low molecular weight atactic-PHB ($M_w = 9400$) in the melt within the atactic-PHB content up to 50 wt.%, and is immiscible with high molecular weight atactic-PHB and commercial-grade bacterial PHB [15,16]. However, to the best of our knowledge, few studies have been reported on the miscibility of PLLA blended with semi-crystalline low molecular weight PHB.

It is noteworthy that blends of PHB and PLLA belong to the family of crystalline/crystalline polymer blends. Thus, the crystallization behavior of each component in the PHB/PLLA blends is dependent on their miscibility, physical properties and crystallization conditions. For example, the crystallization of one component affects the morphology, crystallization, and mechanical properties of the other. According to the study [12], when the

* Corresponding author. Tel.: +81 79 565 8349; fax: +81 79 565 9077.
E-mail address: ozaki@kwansei.ac.jp (Y. Ozaki).

miscible PHB/PLLA blends were cooled from the melt, two types of spherulites were formed, relating to the crystallization of PHB and PLLA, respectively. The radial growth rate of the PHB-type spherulites was strongly dependent on its composition, decreasing when the PLLA content increased. Furthermore, the growth rate was constant for any temperature and composition, suggesting that PLLA component remained in the interlamellar regions of the PHB spherulites, and was not excluded from these spherulites. Park et al. [16] found that the crystallization enthalpy of the PLLA component in the ultra high molecular weight PHB/PLLA blends was lower than in the bacterial PHB/PLLA blends.

Fourier-transform infrared (FTIR) spectroscopy is sensitive to the conformation and local molecular environment of polymers. It has been used as an indispensable and powerful tool for the analysis and characterization of PHB and PLLA due to their distinct IR absorption patterns of amorphous and crystalline components [18–29]. Moreover, IR spectroscopy can be applied to measure compositional variations in phase-separated structures of various polymer blends. It characterizes the crystal formation and the distribution of crystallites within each phase by monitoring changes in characteristic bands [19–21]. For PHB/PLLA blends, the presence or absence of a distinct IR absorption band around 1720 cm^{-1} can be used as a sensitive indicator of the formation of PHB crystals [18]. By using IR microspectroscopy, the spherulitic structures and nonspherulitic parts of PHB/PLLA blends were characterized [19,20]. The results suggested that PHB crystallizes in all the blends, nevertheless, the crystalline structures of PHB in the 80/20, 60/40, 40/60 PHB/PLLA blends were different from that of the 20/80 blend. Recently, by adjusting the molecular weight of PLLA component in PHB/PLLA blends, the stepwise and simultaneous crystallization behavior of the two components in their immiscible and miscible 50/50 blends was investigated by real-time IR spectroscopy [21]. Dynamic analysis disclosed that the crystallization of PLLA proceeded faster than that of PHB in stepwise and simultaneous crystallization. However, the final crystallinities of PLLA were depressed largely by the simultaneous crystallization of PHB [21]. Therefore, it is interesting to investigate the crystallization behavior of one component affected by the other in the PHB/PLLA blends by using IR spectroscopy. In the present study, the miscibility of PLLA blended with a low molecular weight PHB is investigated by differential scanning calorimetry (DSC). It has been found that PLLA shows some limited miscibility with low molecular weight PHB ($M_w = 5000\text{ g mol}^{-1}$) when the PHB content is below 25%. Furthermore, the crystallization and melting behavior of PLLA blended with a small amount of low molecular weight PHB during the heating process are explored by monitoring the changes in characteristic IR bands of each component.

2. Experimental section

2.1. Materials and sample-preparation procedures

Bacterially synthesized PHB ($M_w = 650,000\text{ g mol}^{-1}$ and $M_n/M_w = 2.2$, HMW-PHB) was obtained from the Procter & Gamble Company, Cincinnati, USA. HMW-PHB was purified by first dissolving the sample into hot chloroform, and then precipitating in methanol, and vacuum-drying at $60\text{ }^\circ\text{C}$ for 24 h. PLLA ($M_w = 200,000\text{ g mol}^{-1}$) and low molecular weight PHB ($M_w = 5000\text{ g mol}^{-1}$, LMW-PHB) were obtained from Shimadzu Corporation and Polysciences Inc., respectively. Chloroform and methanol were purchased from Wako Pure Chemical Industries, Ltd, Osaka, Japan.

Blends of PHB and PLLA with various compositions were prepared by dissolving each component together in hot chloroform. The solution of both polymers was cast on a KBr window at room temperature. After the majority of the solvent had been evaporated, the films were placed under vacuum at room temperature for 48 h

to completely remove residual solvent. Blend samples were heated to a temperature at $195\text{ }^\circ\text{C}$ for 2 min to remove any nuclei in them and subsequently quenched into liquid nitrogen to get amorphous samples used for crystallization study.

2.2. DSC measurement

Thermal analysis was carried out with a Perkin Elmer Pyris 6 apparatus, under a nitrogen purge. High purity indium and zinc were used for temperature calibration and indium standard was used for calibration of the heat of fusion (ΔH). The thermogram was obtained by heating quenched specimen from -50 to $200\text{ }^\circ\text{C}$ at a heating rate of $10\text{ }^\circ\text{C min}^{-1}$.

2.3. IR measurement

A KBr window with a blend sample was set on a home made variable temperature cell, which was placed in the sample compartment of a Thermo Nicolet Magna 870 spectrometer equipped with an MCT detector. The spectra of samples were measured at a 2 cm^{-1} spectral resolution with 16 scans coadded. For the crystallization and melting process study, the heating rate of $2\text{ }^\circ\text{C min}^{-1}$ was used.

2.4. WAXD measurement

To investigate the crystalline structure of the blend samples, wide-angle X-ray diffraction measurement was carried out on Rigaku RINT2100 system by using Cu K α radiation ($\lambda = 0.15418\text{ nm}$, 50 kV, 40 mA) in the scattering angle range of $2\theta = 11\text{--}21^\circ$ at a scan speed of $1^\circ/\text{min}$. The temperature was increased at a rate of ca. $2\text{ }^\circ\text{C min}^{-1}$ and WAXD data were recorded at every $10\text{ }^\circ\text{C}$ ranging from 30 to $180\text{ }^\circ\text{C}$. Before each WAXD measurement, the cell was maintained at that temperature for 5 min to make the sample equilibrated.

3. Results and discussion

3.1. DSC analysis of thermal properties of PHB/PLLA blends

The difference in the glass transition temperatures (T_g s) between neat PHB (around $0\text{ }^\circ\text{C}$) and neat PLLA (around $60\text{ }^\circ\text{C}$) is about $60\text{ }^\circ\text{C}$, and then the miscibility can be determined by measuring the T_g of these two components [30]. Fig. 1a and b shows the DSC thermograms of melt-quenched PLLA blended with HMW-PHB and LMW-PHB, respectively. It has been found that neat PLLA exhibits a glass transition around $60\text{ }^\circ\text{C}$, a broad cold-crystallization peak at $100\text{--}150\text{ }^\circ\text{C}$ and a melting peak at about $172\text{ }^\circ\text{C}$. Neat HMW-PHB exhibits a glass transition around $4\text{ }^\circ\text{C}$, meanwhile, a sharp exothermic peak and a melting peak are observed at $50\text{ }^\circ\text{C}$ and $175\text{ }^\circ\text{C}$, respectively, suggesting that PHB crystallizes more rapidly at a lower temperature as compared with PLLA. In a similar manner, LMW-PHB also crystallizes rapidly and yields an exothermic cold-crystallization peak around $50\text{ }^\circ\text{C}$. Expectedly, its melting point is lower than that of HMW-PHB, and double melting peaks appear, suggesting that molecular weight has effect on multiple melting behavior of PHB [31,32].

As can be seen from Fig. 1, the glass transition region of PLLA is very close to the position of the exothermic peak of PHB. Therefore, the confirmation of the occurrence of glass transition temperature (T_g) of PLLA in such blends is rather difficult. However, it is noticed that when PLLA is blended with HMW-PHB, T_g of the PHB component remains almost unchanged over the whole range of the weight fraction of the PLLA component. In addition, two cold-crystallization peaks, respectively, corresponding to HMW-PHB and PLLA components are observed in all the blend samples. The exothermic peak of the PLLA component shifts slightly to higher

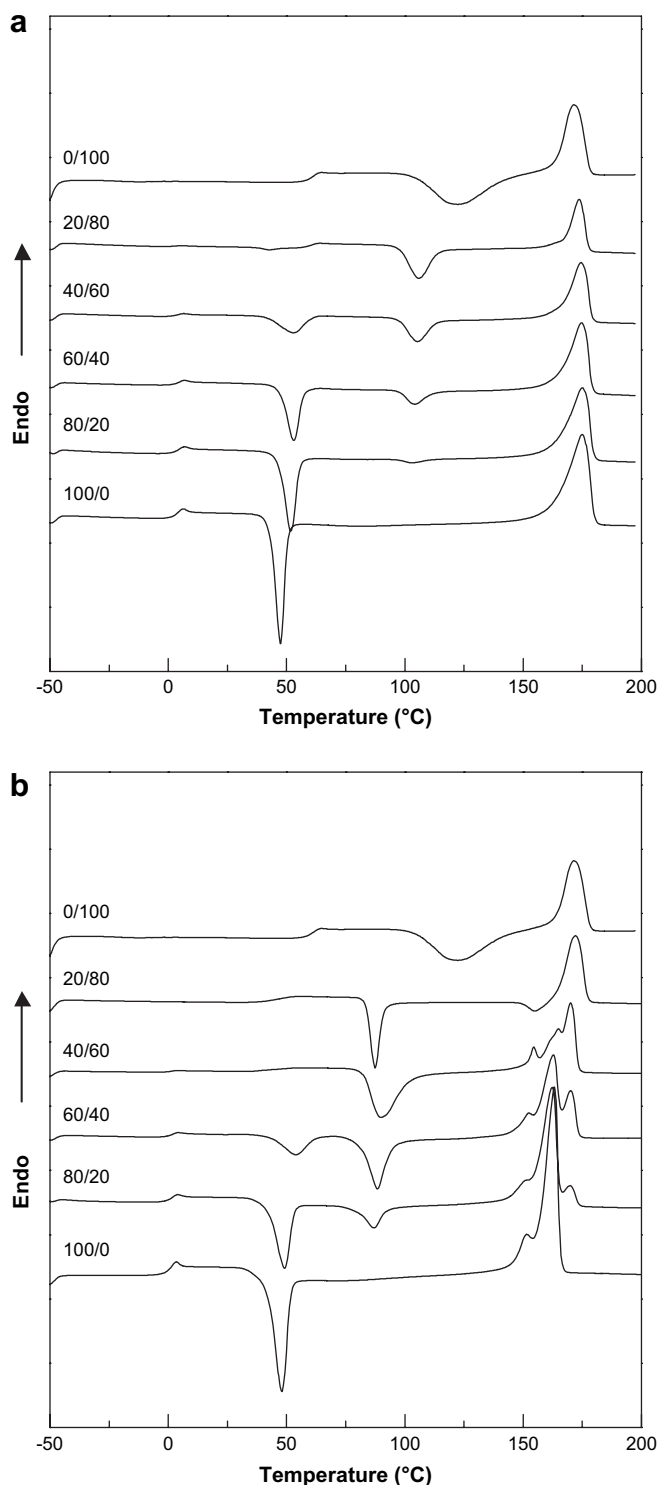


Fig. 1. DSC thermograms of (a) HMW-PHB/PLLA blends and (b) LMW-PHB/PLLA blends obtained from the second heating run with a heating rate of $10\text{ }^{\circ}\text{C min}^{-1}$.

temperature with PHB weight fraction decreasing. These observations suggest that the binary blends are, indeed, immiscible, which is consistent with the results of previous studies [13,14,16]. In the case of LMW-PHB/PLLA blends, with increasing PLLA content up to 60%, the blends show two cold-crystallization peaks as well as one distinct T_g in DSC measurement at about $2\text{ }^{\circ}\text{C}$ which is close to that of neat PHB. Compared with the HMW-PHB/PLLA blends, the cold crystallization of the PLLA component occurs at lower temperature with higher crystallization enthalpy. However, for the LMW-PHB/

PLLA blend of 20/80, only T_g of PLLA can be observed, which is lower compared with that of neat PLLA. Especially, the exothermal cold-crystallization peak of PHB could not be detected, and that of PLLA shifts to lower temperature together with sharper shape. So it is possible that LMW-PHB shows some limited miscibility with PLLA in the LMW-PHB/PLLA 20/80 blend.

For further analysis, the DSC thermograms of melt-quenched PLLA blends with LMW-PHB with its content at every 5% between 5 and 30%, and the corresponding transition temperatures about glass transition (T_g), cold crystallization (T_c) and a small exothermal peak (T_{cs}) of PLLA, respectively, are shown in Figs. 2 and 3. It can be seen that T_g and T_c of PLLA decrease with PLLA fraction changing from 95% to 75%, together with the sharper shape of cold-crystallization peak, which shows different situations with those of PLLA blended with higher LMW-PHB content. Generally, T_c must occur at a temperature above the T_g , where the crystallizable polymer chains possess enough segmental mobility to crystallize. Accordingly, a lower T_g with larger molecular mobility should be accompanied by the lower T_c [33]. A small exothermal peak, labeled as S, appears just below the melting point, and its value also decreases. However, the peak S cannot be observed in the DSC curves of neat PLLA. A recent study by Ling and Spruiell [32] showed that the appearance of this peak depends on a heating rate. It was suggested that at a lower heating rate, the cold crystallization requires longer time to complete, and the crystals formed are more stable. Thus, the onset of melt recrystallization would not strongly compete with the cold crystallization, and recrystallization occurs primarily in the neighborhood of the peak S. On the other hand, at a higher heating rate, the initially formed crystals are less stable and begin to recrystallize immediately during the cold crystallization, yielding as an overall broad peak, but no S peak. In the present study, this peak can be observed even at a higher heating rate ($10\text{ }^{\circ}\text{C/min}$). It suggests that the addition of a small amount of LMW-PHB facilitates the cold crystallization of PLLA, and makes the recrystallization occur just prior to the melting point. The above results suggest that LMW-PHB shows some limited miscibility with PLLA when

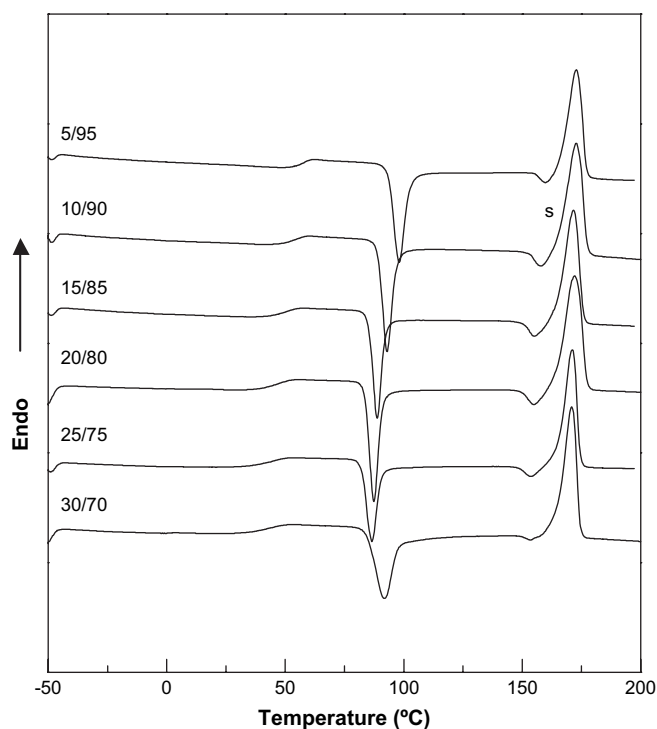


Fig. 2. DSC thermograms of PLLA blended with a small amount of LMW-PHB obtained from the second heating run with a heating rate of $10\text{ }^{\circ}\text{C min}^{-1}$.

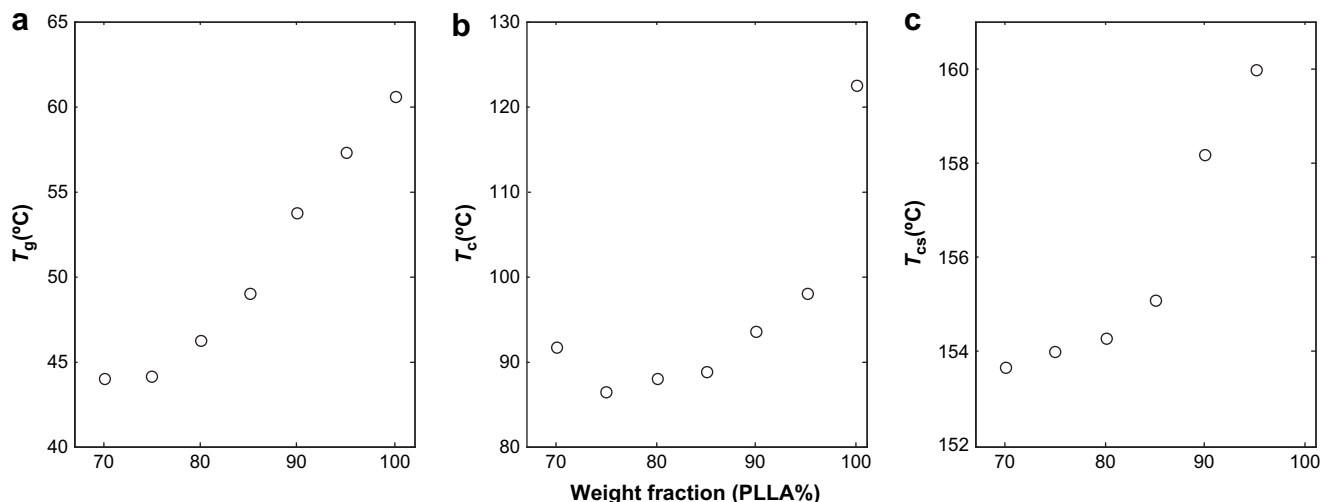


Fig. 3. Transition temperatures of (a) T_g , (b) T_c , and (c) T_{cs} as a function of PLLA weight fraction obtained from Fig. 2.

LMW-PHB content is at or below 25%, whereas LMW-PHB shows no miscibility with PLLA in the amorphous state for the blends containing PHB content higher than 30%. According to the previous studies [12–14], PLLA with low molecular weight (below $M_w = 18,000$) was miscible with PHB in the melt state over the whole composition range. On the other hand, PLLA and low molecular weight atactic-PHB ($M_w = 9400$) are miscible in the melt at 200°C within the atactic-PHB content up to 50 wt.% [15]. Comparison with these studies suggests that the miscibility in PHB/PLLA blends is not strongly dependent on the molecular weight of semicrystallizable PHB.

3.2. Composition-dependent IR spectra of LMW-PHB/PLLA blends

Fig. 4 shows FTIR spectra of LMW-PHB/PLLA blends with various PHB contents solvent-cast and crystallized at room temperature in the regions of $1810\text{--}1660$ and $1500\text{--}800\text{ cm}^{-1}$. PHB and PLLA are semi-crystalline polymers, and thus their spectral profiles are greatly affected by their corresponding physical states and crystalline structures. For PHB, the bands at 1740 and 1723 cm^{-1} are, respectively, ascribed to the C=O stretching modes of the amorphous and crystalline parts, those bands at 1291 , 1279 , and 1263 cm^{-1} are ascribed to the stretching vibrations of the C–O–C groups, and the band at 1228 cm^{-1} due to the CH_2 wagging and

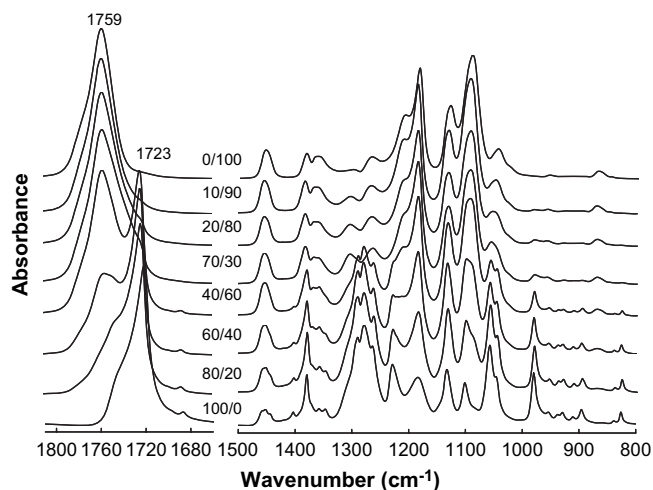


Fig. 4. FTIR spectra of LMW-PHB/PLLA blends with various compositions measured at room temperature in the regions $1810\text{--}1660\text{ cm}^{-1}$ and $1500\text{--}800\text{ cm}^{-1}$.

twisting modes [22–25]. As for PLLA, the band around 1759 cm^{-1} is assigned to the C=O stretching mode [26]. In this sample-preparation conditions, PLLA remains in the amorphous state, while PHB is in the semi-crystalline state. It is interesting to note that, in the blends with compositions of LMW-PHB/PLLA = 80/20–40/60, the crystalline sensitive bands of PHB dominates, for example, those at 1723 , 1291 , 1279 , 1263 , and 1228 cm^{-1} , even though their intensities decrease. Nevertheless, the amorphous bands of PLLA dominate for the LMW-PHB/PLLA = 30/70–10/90 blends, indicating that the crystallinity of the blends decreases as the PLLA content increases. Although there are some overlapping of C=O stretching bands between PHB and PLLA, the crystalline band of PHB centered around 1723 cm^{-1} can be used as an indicator of the formation of PHB crystals. As can be seen from Fig. 4, an abrupt decrease in the intensity of the crystalline C=O band of PHB occurs when the composition of the LMW-PHB content is equal to or below 30%. However, the appearance of this band still can be detected from the original spectra, which indicates that PHB can crystallize even at a relatively low content when the blends are prepared by solvent casting. Besides the band at 1723 cm^{-1} , there are also a number of C–C stretching bands located in the $1000\text{--}800\text{ cm}^{-1}$ region which can also be used to indicate the spectral variations with blend composition changes. An obvious peak shift or an appearance of a new band cannot be detected in the IR spectra of these blends, suggesting that it is not a strong inter- or intramolecular interaction that causes the partial miscibility between the LMW-PHB/PLLA blends.

3.3. Nonisothermal crystallization and subsequent melting behavior

It is interesting to investigate how the two components of the blends crystallize, and how the crystallization of one component influences the other since both of them are semicrystallizable polymers. As described above, the crystallization and melting behavior of each component in LMW-PHB/PLLA blends can be investigated by monitoring changes in the characteristic IR bands. Fig. 5 shows IR spectra of PLLA blended with 0%, 10%, 20% and 30% of LMW-PHB contents measured at room temperature. These blend samples were prepared by first melting, followed by quenching in liquid nitrogen, and then their IR spectra measured at room temperature. One can easily see that the crystalline band of PHB at 1723 cm^{-1} cannot be observed, suggesting that it is difficult for a small amount of PHB to crystallize in the quenched sample blends. It turns out that PHB particles in the PLLA matrix at low levels are not crystallized and remain in the amorphous state at room temperature [18].

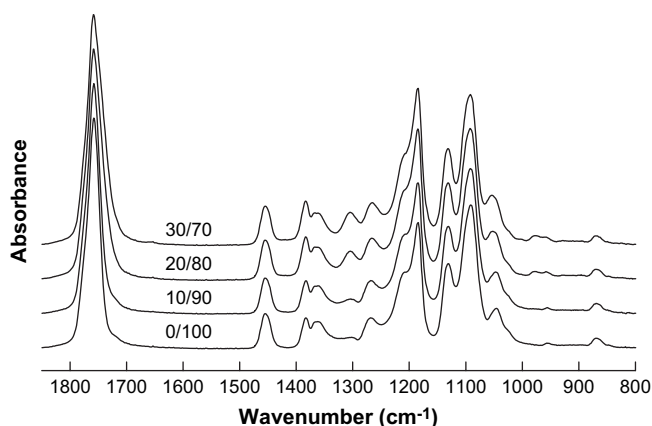


Fig. 5. IR spectra in the region $1850\text{--}800\text{ cm}^{-1}$ of quenched LMW-PHB/PLLA blends with various blend ratios measured at room temperature.

The thermal behavior of each component in the blends with varying temperature was further investigated by real-time FT-IR spectroscopy. Fig. 6 displays temperature-dependent IR spectra of PHB (a, b) and LMW-PHB/PLLA 20/80 blend (c, d) in the range of $1820\text{--}1680\text{ cm}^{-1}$ collected during the heating process from 35 to $185\text{ }^{\circ}\text{C}$ at a heating rate of $2\text{ }^{\circ}\text{C min}^{-1}$. In this spectral region, the characteristic C=O stretching bands of PLLA and PHB around 1759 and 1723 cm^{-1} , respectively, are very sensitive to their crystal

structure. Obviously, the appearance of the band at 1723 cm^{-1} suggests that the crystallization of PHB occurs in the blends during the heating process. Therefore, the structural changes of each component in the blends during the heating process can be monitored by plotting the normalized intensity changes of the C=O bands at 1759 and 1723 cm^{-1} obtained from the difference spectra as a function of temperature, as depicted in Fig. 7a and b. It is easy to see that the intensity changes of $\nu(\text{C}=\text{O})$ band at 1759 cm^{-1} (Fig. 7a) show similar trends for different samples with various LMW-PHB fractions, which reflect the complex thermal behavior of PLLA in the blends. Firstly, the intensity of the band at 1759 cm^{-1} slightly detrends in the temperature of $40\text{--}60\text{ }^{\circ}\text{C}$ for the LMW-PHB/PLLA 20/80 and 30/70 blend samples, and $60\text{--}80\text{ }^{\circ}\text{C}$ for neat PLLA and the 10/90 blend sample. Taking into consideration the previous DSC results and other works [34,35], such an intensity change may be attributed to the glass transition of PLLA. Secondly, there is an obvious increase in the intensity of the band at 1759 cm^{-1} in the temperature range from 65 to $95\text{ }^{\circ}\text{C}$. This result strongly suggests that the cold crystallization of PLLA occurs here. Interestingly, as the PHB fraction increases in the blends, the starting temperature of cold crystallization shifts to a lower temperature, but it shows little change when the PHB content is further increased up to 30%. This indicated that the addition of a small amount of PHB component (i.e., 10 and 20%) facilitated the occurrence of PLLA cold crystallization in the binary blends. Finally, there is an obvious transition of the C=O band in the temperature range from 150 to $165\text{ }^{\circ}\text{C}$. In this temperature range, the intensity of

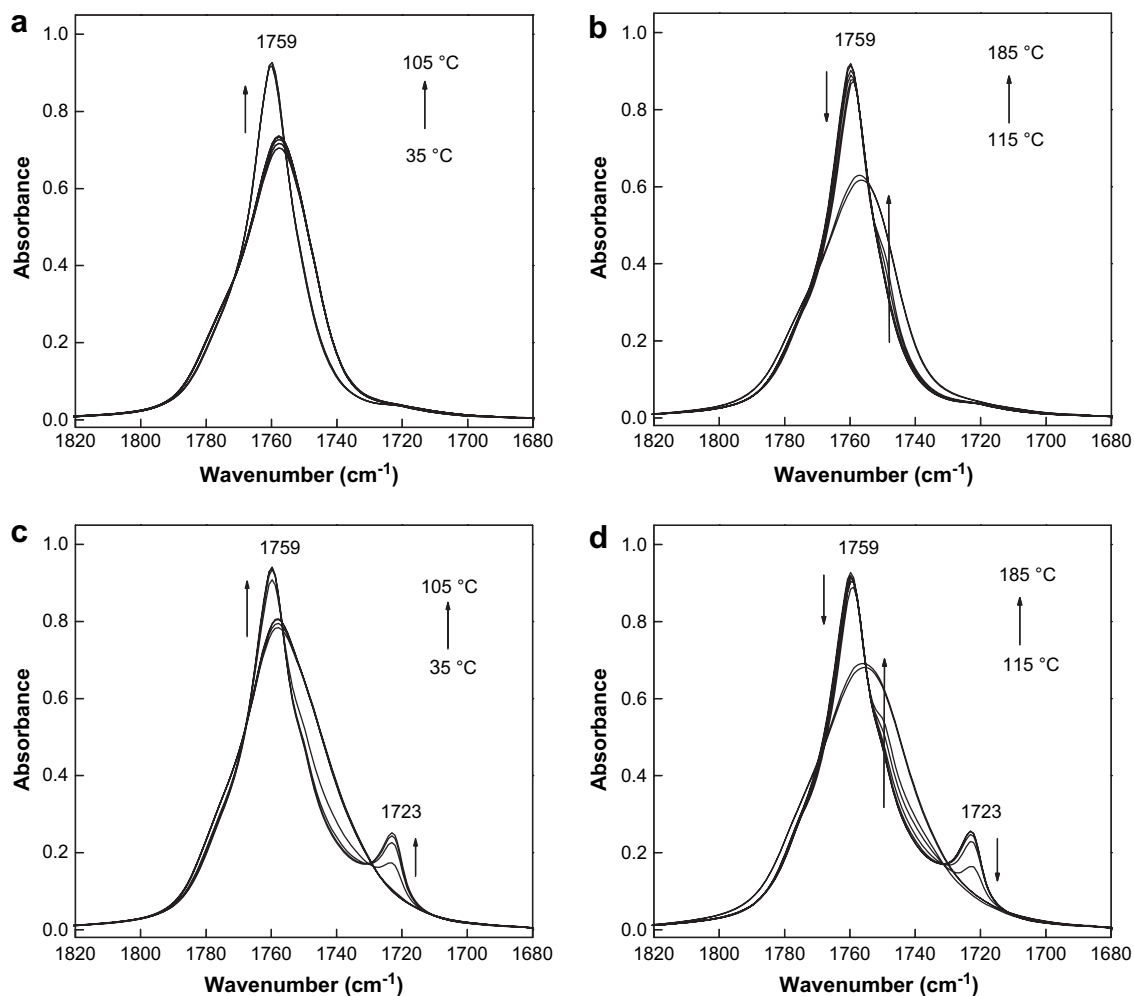


Fig. 6. FTIR spectra in the range $1850\text{--}1650\text{ cm}^{-1}$ of (a, b) PLLA and (c, d) LMW-PHB/PLLA 20/80 blend collected during heating from 35 to $185\text{ }^{\circ}\text{C}$ at an interval of $10\text{ }^{\circ}\text{C}$.

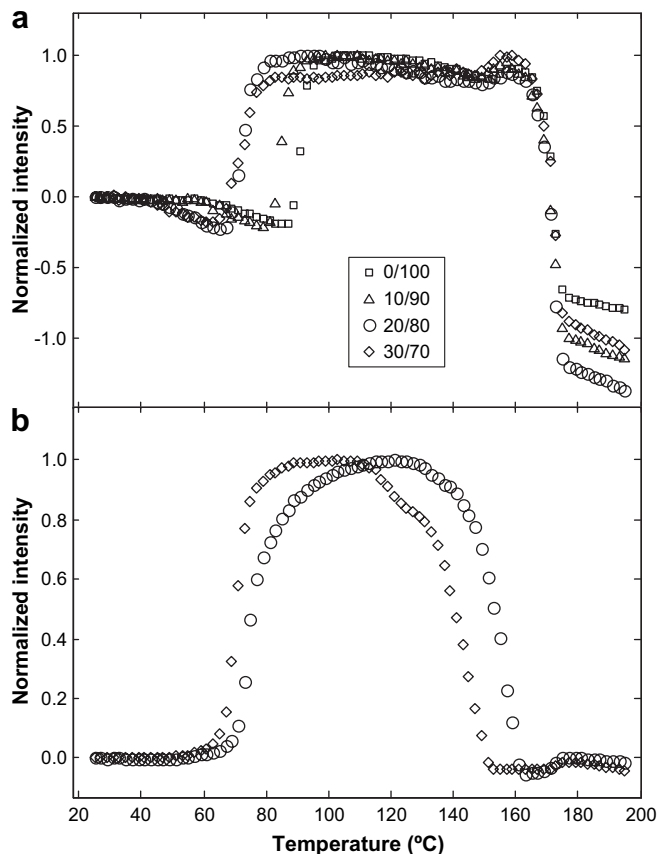


Fig. 7. Normalized intensity changes of the $\nu(\text{C}=\text{O})$ bands at (a) 1759 cm^{-1} and (b) 1723 cm^{-1} as a function of temperature in the heating process of LMW-PHB/PLLA blends with various PHB contents.

the band at 1759 cm^{-1} abruptly shows a clear deviation, strongly suggesting that the recrystallization or phase transition occurs here. Subsequently, the enormous spectral changes occur when the sample is heated from 165 to $175\text{ }^\circ\text{C}$ as shown in Fig. 7a, suggesting the melting of PLLA crystals. As for the transition occurring from 150 to $165\text{ }^\circ\text{C}$, it corresponds to the small exothermic peak in the DSC curve detected just prior to the melting peak of PLLA [27]. Recently, Zhang et al. [27,28,36,37] carried out a series of studies on the thermal behavior of isothermally crystallized PLLA samples at different crystallization temperatures. They suggested that the exotherm is associated with the first-order-type disorder-to-order (α' -to- α) phase transition based on the WAXD, DSC and IR analysis results. Considering these results, it is postulated that α' crystals of PLLA are formed during the heating of PHB/PLLA blends.

For further analysis of PLLA crystal formation, Fig. 8a and b exhibits the WAXD profiles of quenched PLLA and LMW-PHB/PLLA 20/80 blend samples measured every $10\text{ }^\circ\text{C}$ in the heating process from 30 to $180\text{ }^\circ\text{C}$. The WAXD profiles measured at $30\text{ }^\circ\text{C}$ clearly reflect that both PHB and PLLA are in the amorphous state. As can be seen from Fig. 8a, as temperature increases to $80\text{ }^\circ\text{C}$, the two reflections of 200/110 and 203 are observed, indicating the formation of PLLA crystals. Besides these two reflections of PLLA crystal, the reflection of 020 is observed for the 20/80 blend, suggesting the formation of PHB crystals. For both samples, with increasing temperature prior to $150\text{ }^\circ\text{C}$, the peak position of the observed reflections shifts to lower angle side due to the thermal expansion of the lattice. In the temperature ranging from 150 to $160\text{ }^\circ\text{C}$, the 200/110 and 203 reflections shift remarkably toward the higher angle. Referring to the literature [37], the result demonstrates that there is a first-order transition of the two phases (α' -to- α)

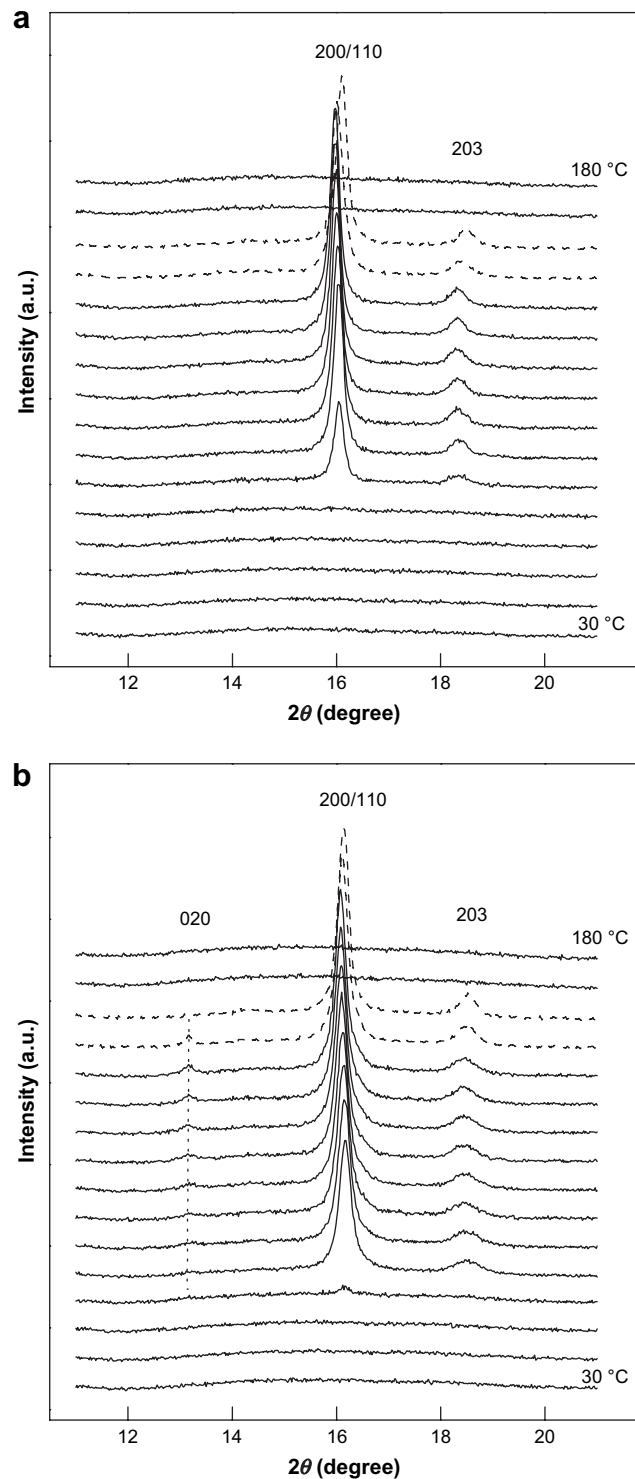


Fig. 8. Temperature-dependent WAXD profiles of (a) PLLA and (b) LMW-PHB/PLLA = 20/80 blend collected in the heating process from 30 to $180\text{ }^\circ\text{C}$ at an interval of $10\text{ }^\circ\text{C}$.

in this temperature range. The WAXD results are in agreement with the present IR results. Furthermore, the appearance of two reflections of PLLA crystal is observed at $70\text{ }^\circ\text{C}$ for the 20/80 blend, suggesting that the crystal formation of PLLA in the 20/80 blend occurs at a lower temperature than that of neat PLLA.

The thermal behavior of PHB can also be monitored by the intensity changes of the band at 1723 cm^{-1} , as shown in Fig. 7b. It is found that the cold crystallization of PHB occurs only in the 20/80

and 30/70 blends during the heating process, suggesting that the crystals of PHB and PLLA coexist in them. With the increase in the PHB content, the starting temperature of cold crystallization of PHB shows a little shift to a lower temperature. It is noticed that for the 20/80 blend, the crystallization of PHB and PLLA occur almost simultaneously, nevertheless, that of PHB occurs prior to that of PLLA for the 30/70 blend. In the subsequent melting behavior, the melting of PHB crystals in the 30/70 blend occurs prior to that in 20/80 blend. Similar to PLLA, the intensity of the band at 1723 cm^{-1} shows a clear deviation around $127\text{ }^{\circ}\text{C}$ for 30/70 blend, suggesting that the recrystallization process occurs here.

4. Conclusions

The miscibility, crystallization and melting behavior of LMW-PHB/PLLA blends were investigated by DSC, IR spectroscopy and WAXD. The results of DSC, especially the change in the glass transition temperature of PLLA and the remarkable changes of crystallization behavior of PLLA, have suggested that PLLA shows some limited miscibility with LMW-PHB when the PHB content was below 25%. During the nonisothermal crystallization, the addition of LMW-PHB yields a remarkable effect on the cold crystallization of PLLA in the blends, especially when the PHB content is relatively low. For the 20/80 and 30/70 blends, two crystals, corresponding to the crystallization of PHB and PLLA, were observed by monitoring the intensity changes of individual characteristic IR bands of each component in the heating process. Additionally, for all the samples, the disorder (α') phase of PLLA was produced in the nonisothermal crystallization process, which was supported by an obvious transition associated with the first-order-type disorder-to-order (α' -to- α) transition occurring around $160\text{ }^{\circ}\text{C}$.

Acknowledgements

This work was partially supported by "Open Research Center" project for private universities: matching fund subsidy from MEXT (Ministry of Education, Culture, Sports, Science and Technology), 2001–2008. This work was also supported by Kwansai-Gakuin University "Special Research" project, 2004–2008.

References

- [1] Doi Y. Microbial polyester. New York: VCH; 1990.
- [2] Babel W, Steinbüchel A. Advances in biochemical engineering/biotechnology: biopolyesters. Berlin, Heidelberg, New York: Springer-Verlag; 2001.
- [3] Doi Y, Steinbüchel A. Polyesters II: properties and chemical synthesis. In: Biopolymers, vol. 3b. Wienheim: Wiley-VCH; 2004.
- [4] Iwata T, Doi Y. Macromol Chem Phys 1999;200:2429–42.
- [5] Vert M. Biomacromolecules 2005;6:538–46.
- [6] Sudesh K, Abe H, Doi Y. Prog Polym Sci 2000;25:1503–55.
- [7] Di Lorenzo ML, Raimo M, Cascone E, Martuscelli E. J Macromol Sci Phys B 2001;40:639–67.
- [8] Ha CS, Cho WJ. Prog Polym Sci 2002;27:759–809.
- [9] He Y, Asakawa N, Inoue Y. Polym Int 2000;49:609–17.
- [10] Qiu Z, Ikehara T, Nishi T. Polymer 2003;44:2503–8.
- [11] Huang H, Hu Y, Zhang J, Sato H, Zhang H, Noda I, et al. Phys Chem B 2005;109:19175–83.
- [12] Blümm E, Owen AJ. Polymer 1995;36:4077–81.
- [13] Koyama N, Doi Y. Polymer 1997;38:1589–93.
- [14] Yoon JS, Lee WS, Kim KS, Chin IJ, Kim MN, Kim C. Eur Polym J 2000;36:435–42.
- [15] Ohkoshi I, Abe H, Doi Y. Polymer 2000;41:5985–92.
- [16] Park JW, Doi Y, Iwata T. Biomacromolecules 2004;5:1557–66.
- [17] Furukawa T, Sato H, Murakami R, Zhang J, Noda I, Ochiai S, et al. Polymer 2006;47:3132–40.
- [18] Noda I, Satkowski MM, Dowrey AE, Marcott C. Macromol Biosci 2004;4:269–75.
- [19] Furukawa T, Sato H, Murakami R, Zhang J, Duan YX, Noda I, et al. Macromolecules 2005;38:6445–54.
- [20] Furukawa T, Sato H, Murakami R, Zhang J, Noda I, Ochiai S, et al. Polymer 2007;48:1749–55.
- [21] Zhang J, Sato H, Furukawa T, Tsuji H, Noda I, Ozaki Y. J Phys Chem B 2006;110:24463–71.
- [22] Bloembergen S, Holden DA, Hamer GK, Bluhm TL, Marchessault RH. Macromolecules 1986;19:2865–71.
- [23] Xu J, Guo BH, Yang R, Wu Q, Chen GQ, Zhang ZM. Polymer 2002;43:6893–9.
- [24] Sato H, Murakami R, Padermshoke A, Hirose F, Senda K, Noda I, et al. Macromolecules 2004;37:7203–13.
- [25] Zhang J, Sato H, Noda I, Ozaki Y. Macromolecules 2005;38:4274–81.
- [26] Zhang J, Tsuji H, Noda I, Ozaki Y. Macromolecules 2004;37:6433–9.
- [27] Zhang J, Duan Y, Sato H, Tsuji H, Noda I, Yan S, et al. Macromolecules 2005;38:8012–21.
- [28] Zhang J, Tashiro K, Domb AJ, Tsuji H. Macromol Symp 2006;242:274–8.
- [29] Gao Y, Kong L, Zhang L, Gong Y, Chen G, Zhao N, et al. Eur Polym J 2006;42:764–75.
- [30] Qiu Z, Komura M, Ikehara T, Nishi T. Polymer 2003;44:7749–56.
- [31] Yasuniwa M, Satou T. J Polym Sci Part B Polym Phys 2002;40:2411–20.
- [32] Ling XY, Spruiell JE. J Polym Sci Part B Polym Phys 2006;44:3200–14.
- [33] Chiu HJ. J Appl Polym Sci 2006;100:980–8.
- [34] Qian R, Shen D, Sun F, Wu L. Macromol Chem Phys 1996;197:1485–93.
- [35] Ogura K, Kawamura S, Sobue H. Macromolecules 1971;4:79–81.
- [36] Zhang J, Tashiro K, Tsuji H, Domb AJ. Macromolecules 2007;40:1049–54.
- [37] Zhang J, Tashiro K, Tsuji H, Domb AJ. Macromolecules 2008;41:1352–7.